

Probing a polymerized black hole with the frequency shifts of photons

Qi-Ming Fu^{1, 2, *} and Xin Zhang^{1, 3, 4, †}

¹*Key Laboratory of Cosmology and Astrophysics (Liaoning Province),
College of Sciences, Northeastern University, Shenyang 110819, China*

²*Institute of Physics, Shaanxi University of Technology, Hanzhong 723000, China*

³*Key Laboratory of Data Analytics and Optimization for Smart Industry (Ministry of Education),
Northeastern University, Shenyang 110819, China*

⁴*National Frontiers Science Center for Industrial Intelligence and Systems Optimization,
Northeastern University, Shenyang 110819, China*

As is well-known, black hole plays an important role in probing the quantum effects of gravity in the strong-field regime. In this paper, we focus on a polymerized black hole and investigate the quantum effects on the redshift, blueshift and gravitational redshift of photons emitted by massive particles revolving around this black hole. With a general relativistic formalism, we obtain two elegant and concise expressions for the mass of the black hole and the quantum parameter in terms of few direct observables, and find that all the frequency shifts of photons decrease with the quantum parameter. Besides, we first study the effects of the plasma on the redshift/blueshift, and conclude that the presence of plasma results in the decrease of the redshift/blueshift.

I. INTRODUCTION

Although general relativity has been proven to be very successful in modern physics, it may not be the final theory of gravity because of its prediction of spacetime singularity inside a black hole or at the start of the universe, which indicates that the theory invalidates there. It is widely believed that the singularity can be avoided by incorporating the quantum effects. Many efforts have been devoted to address these issues by resorting to the quantum theory of gravity. One of the most successful attempts is to apply an effective approach developed in loop quantum gravity to the big-bang singularity in cosmological scenarios, where the singularity is replaced by a quantum bounce bridging a contracting branch with an expanding one [1, 2]. The key point is the phase space quantization usually called polymerization [3]. This quantization procedure introduces a natural cutoff called the polymer scale, where the quantum effects become relevant close to this scale.

In recent years, similar technique has been extended to the context of black holes, and a lot of polymerized black hole models have been constructed [4–19]. Most of these models focused on the spherically symmetric cases. The common feature of these types of models is that the singularity inside a black hole is replaced by a space-like transition hypersurface, which smoothly connects a trapped region (the black hole region) to an anti-trapped region (the white hole region), and the spacetime is regular everywhere. Besides, the resulting spacetime with the quantum corrections can still be described by an explicit metric. Thus, one can investigate such nonsingular models by exploiting the already well-developed mechanism

for the semiclassical black holes.

In the last couple of years, various aspects of the polymerized black holes have been studied in the literature. For example, the role of Dirac observables in polymerized black hole models was investigated in Ref. [19], and the interior structure, quasinormal spectra of various perturbation modes were studied in Ref. [20]. The thermodynamic properties of the polymerized black holes were analyzed in Ref. [21], and the effects of the quantum corrections on the relevant thermodynamic quantities also were considered. In addition, the Hawking radiation emitted by polymerized black holes for the fields with different spins were investigated in Refs. [22, 23], and the authors also investigated the primordial black hole evaporation signals with the Hawking radiation rates. Recently, the strong gravitational lensing of the polymerized black holes was investigated in Ref. [24], and the solar system experiments of these black holes were considered in Ref. [25], from which the constraints on the polymer scale were derived as well. Other phenomenological investigations and observational constraints on the polymerized black holes were explored in Refs. [26–32] and references therein. In this paper, we mainly concentrate on the polymerized black hole introduced in Refs. [18, 19] and investigate the frequency shifts of the photons emitted by massive objects orbiting this black hole.

On the other hand, the authors of Ref. [33] introduced a general relativistic method that can express the mass and spin of a Kerr black hole in terms of direct observables, i.e., the radius of the massive particles orbiting the black hole and the frequency shifts experienced by the photons emitted by these revolving particles. Subsequently, this general relativistic mechanism was applied to other black holes, such as, Myers-Perry black hole [34], Kerr-Newman-(anti) de Sitter black hole [35], and Plebanski-Demianski black hole [36]. Besides, the redshift and blueshift of photons emitted by timelike geodesic particles near compact objects, such as, boson star, as well as the Schwarzschild and Reissner-

*fuqiming@sut.edu.cn

†Corresponding author.
zhangxin@mail.neu.edu.cn

Nordström black holes were investigated in Ref. [37]. In Refs. [38, 39], a similar formalism was used to obtain the relations between the parameters describing a class of regular black holes and the redshift observables. Other investigations on the frequency shifts of photons can be found in Refs. [40–45].

Although the polymerized black hole has been extensively studied in the literature, the frequency shifts of photons emitted by massive particles orbiting this black hole have not been analyzed yet. With the general relativistic formalism, one can obtain closed formulas for the mass and the quantum parameter of the polymerized black hole in terms of the frequency shifts of the emitted photons. Thus, this mechanism not only provides us with valuable information about the black hole with few direct observables, but also can be used as a powerful tool to probe the quantum effects. On the other hand, most astrophysical black holes in nature are surrounded by a plasma medium and the frequency of photons will be influenced by the plasma [46–48]. Thus, it is necessary to study the polymerized black hole with the general relativistic formalism and it is also of interest to know what the effects are of the plasma on the frequency shifts.

This paper is organized as follows. In Sec. II, we first give a brief review of the polymerized black hole and then derive the equations of motion for the orbiting massive particles and the photons emitted by these particles. In Sec. III, we investigate the frequency shifts of the photons and derive the closed formulas for the mass and quantum parameter of the black hole. The effects of the plasma on the frequency shifts are analyzed in Sec. IV. Section V comes with the conclusion.

II. PARTICLES AND PHOTONS IN A POLYMERIZED BLACK HOLE SPACETIME

The static and spherically symmetric metric modified by the effective loop quantum gravity can be expressed as [18, 19, 26]:

$$ds^2 = -\mathcal{A}(y)d\tau^2 + \frac{dy^2}{\mathcal{A}(y)} + \mathcal{C}^2(y)d\Omega_2^2, \quad (1)$$

where the radial coordinate $y \in (-\infty, \infty)$, and the metric functions are given by

$$\mathcal{A}(y) = \left(1 - \frac{1}{\sqrt{2A_\lambda(1+y^2)}}\right) \frac{1+y^2}{\mathcal{C}^2(y)}, \quad (2)$$

$$\mathcal{C}^2(y) = \frac{A_\lambda}{\sqrt{1+y^2}} \frac{M_B^2(y+\sqrt{1+y^2})^6 + M_W^2}{(y+\sqrt{1+y^2})^3}. \quad (3)$$

Here M_B and M_W represent the masses of an asymptotically Schwarzschild black hole and a white hole, respectively [26], and A_λ is a dimensionless and non-negative parameter defined by $A_\lambda \equiv (\lambda_k/(M_B M_W))^{2/3}/2$, where λ_k is a quantum parameter originated from holonomy

modifications [18, 19]. In this paper, we focus on the case of $M_B = M_W = M$ corresponding to a symmetric bounce, i.e., the spacetime is symmetric under $y \rightarrow -y$. Without loss of generality, we focus on the positive branch with $y \geq 0$. By redefining two new coordinates $r \equiv \sqrt{8A_\lambda M}y$ and $t \equiv \tau/(\sqrt{8A_\lambda M})$, the metric (1) can be reexpressed as [24, 26]

$$ds^2 = -A(r)dt^2 + B(r)dr^2 + C(r)(d\theta^2 + \sin^2\theta d\phi^2), \quad (4)$$

where

$$A(r) = \frac{1}{B(r)} = \frac{\sqrt{8A_\lambda M^2 + r^2}(\sqrt{8A_\lambda M^2 + r^2} - 2M)}{2A_\lambda M^2 + r^2}, \quad (5)$$

$$C(r) = 2A_\lambda M^2 + r^2. \quad (6)$$

The event horizon of this black hole is determined by $A(r) = 0$, which admits the solution $r = 2M\sqrt{1-2A_\lambda}$. Hence the permissible range for the quantum parameter A_λ in this black hole spacetime is $0 \leq A_\lambda \leq \frac{1}{2}$.

The Lagrangian for a massive particle moving around this black hole is

$$2\mathcal{L} = -A(r)\dot{t}^2 + B(r)\dot{r}^2 + C(r)(\dot{\theta}^2 + \sin^2\theta\dot{\phi}^2), \quad (7)$$

where $\dot{x}^\mu = U^\mu \equiv \frac{dx^\mu}{d\tau}$, U^μ denotes the four velocity of the massive particle, and τ is an affine parameter along the geodesic. Since the Lagrangian only depends on r and θ , there appear two conserved quantities along the geodesic:

$$p_t = \frac{\partial \mathcal{L}}{\partial \dot{t}} = -A(r)\dot{t} = -A(r)U^t = -E, \quad (8)$$

$$p_\phi = \frac{\partial \mathcal{L}}{\partial \dot{\phi}} = C(r)\sin^2\theta\dot{\phi} = C(r)\sin^2\theta U^\phi = L, \quad (9)$$

which correspond to the energy and angular momentum of the massive particle with unit rest mass, respectively. From the normalized condition $U_\mu U^\mu = -1$, the geodesic equation for the massive particle at the equatorial plane ($U^\theta = 0$) can be derived as

$$(U^r)^2 + V(r) = 0, \quad (10)$$

with the effective potential

$$V(r) = \frac{1}{B} \left(1 - \frac{E^2}{A} + \frac{L^2}{C}\right). \quad (11)$$

For circular orbits, i.e., $U^r = 0$, the effective potential must have an extremum indicating two conditions $V(r) = 0$ and $V'(r) = 0$, where the prime stands for the derivative with respect to r . From these two conditions, one can obtain

$$E^2 = \frac{A^2 C'}{AC' - CA'}, \quad (12)$$

$$L^2 = \frac{C^2 A'}{AC' - CA'}. \quad (13)$$

Besides, for the circular orbits to be stable, the following stable condition should also be satisfied:

$$V'' = \frac{C'(2AA'C' + C(AA'' - 2A'^2)) - ACA'C''}{ABC(AC' - CA')} > 0. \quad (14)$$

Inserting Eqs. (12) and (13) into Eqs. (8) and (9), the four-velocity for the circular and equatorial orbiting massive particles can be calculated as

$$U^t = \sqrt{\frac{C'}{AC' - CA'}}, \quad (15)$$

$$U^\phi = \sqrt{\frac{A'}{AC' - CA'}}. \quad (16)$$

On the other hand, the energy and angular momentum for the photons moving along null geodesics can be obtained in a similar way:

$$E_\gamma = Ak^t, \quad L_\gamma = Ck^\phi, \quad (17)$$

with $k^\mu = (k^t, k^r, k^\theta, k^\phi)$ the four momentum of the photons, which satisfies $k^\mu k_\mu = 0$. Then, the equation of motion for the photons at the equatorial plane is

$$-A(k^t)^2 + B(k^r)^2 + C(k^\phi)^2 = 0. \quad (18)$$

After inserting Eq. (17) into the above equation, the radial component of the four momentum can be solved as

$$(k^r)^2 = \frac{-AL_\gamma^2 + CE_\gamma^2}{ABC}. \quad (19)$$

Introducing an auxiliary bidimensional and geometrical vector defined by $\kappa^2 \equiv (k^r)^2 + C(k^\phi)^2$, where the components k^r and k^ϕ satisfy the following decomposition [45]:

$$k^r = \kappa \cos \phi, \quad (20)$$

$$\sqrt{C}k^\phi = \kappa \sin \phi, \quad (21)$$

with $0 \leq \phi \leq 2\pi$, the auxiliary vector can be explicitly expressed as

$$\kappa^2 = \frac{-AL_\gamma^2 + CE_\gamma^2}{ABC} + C \left(\frac{L_\gamma}{C} \right)^2. \quad (22)$$

Besides, after inserting Eq. (20) into Eq. (19), another expression for the auxiliary vector can be obtained as

$$\kappa^2 = \frac{-AL_\gamma^2 + CE_\gamma^2}{ABC \cos^2 \phi}. \quad (23)$$

Combining these two expressions (22) and (23) for the auxiliary vector together, one can obtain an equation for the impact parameter $b \equiv \frac{E_\gamma}{L_\gamma}$:

$$b^2 A(\sin^2 \phi + B \cos^2 \phi) - C \sin^2 \phi = 0, \quad (24)$$

which admits the following solution

$$b = -\frac{\sqrt{C} \sin \phi}{\sqrt{A(\sin^2 \phi + B \cos^2 \phi)}}. \quad (25)$$

The maximum or minimum of the impact parameter is reached when $k^r = 0$ corresponding to $\phi = -\pi/2$ or $\pi/2$, respectively.

III. REDSHIFT/BLUESHIFT OF EMITTED PHOTONS

The frequency shift of a photon emitted by a massive particle moving around a black hole and then received by a detector can be defined as [33]

$$1 + z = \frac{\omega_e}{\omega_d} = \frac{-k_\mu U^\mu|_e}{-k_\mu U^\mu|_d}, \quad (26)$$

where the lower indexes e and d represent the emitter and detector, respectively. For the case of a circular and equatorial orbiting massive particle, i.e., $U^r = U^\theta = 0$, Eq. (26) can be reduced to

$$1 + z = \frac{(E_\gamma U^t - L_\gamma U^\phi)|_e}{(E_\gamma U^t - L_\gamma U^\phi)|_d} = \frac{U_e^t - b_e U_e^\phi}{U_d^t - b_d U_d^\phi}. \quad (27)$$

There are mainly two contributions to the frequency shift defined above, i.e., the gravitational effect and the kinematic effect or Doppler effect. The impact parameter for a radially emitted photon is usually called the central impact parameter b_c , which vanishes for a spherically symmetric and static black hole, and the only contribution to the frequency shift of this photon is the gravitational effect. Thus, the gravitational redshift can be conveniently defined as [37]

$$1 + z_g = \frac{U_e^t - b_c U_e^\phi}{U_d^t - b_c U_d^\phi} = \frac{U_e^t}{U_d^t}. \quad (28)$$

Then, the kinematic redshift z_{kin} originated from the kinematic effect of the emitter can be defined by subtracting the gravitational redshift z_g from the frequency shift z [37]:

$$z_{\text{kin}} \equiv z - z_g = \frac{U_e^t - b_e U_e^\phi}{U_d^t - b_d U_d^\phi} - \frac{U_e^t}{U_d^t}. \quad (29)$$

Besides, if there is a relative motion of the black hole with respect to a distant observer or detector, there should be an additional correction to the frequency shifts of photons coming from the special relativistic boost, which is defined by [45]

$$1 + z_{\text{boost}} = \gamma(1 + \beta), \quad \gamma = (1 - \beta^2)^{-1/2}, \quad \beta = \frac{v_0}{c}, \quad (30)$$

where $v_0 = z_0 c$ represents the radial peculiar velocity of the black hole with respect to the observer, and z_0 is called the peculiar redshift which codifies the motion of the black hole receding (positive z_0) or approaching (negative z_0) with respect to the observer. Then, by considering Eqs. (15), (16) and (25), the total frequency shift can be expressed as [45]

$$\begin{aligned} z_{\text{tot}} &= (1 + z)(1 + z_{\text{boost}}) - 1 \\ &= (1 + z_{\text{kin}} + z_g)\gamma(1 + \beta) - 1 \end{aligned}$$

$$\begin{aligned}
&= \sqrt{\frac{1+z_0}{1-z_0}} \left(\sqrt{\frac{C'(r_e)}{A(r_e)C'(r_e) - C(r_e)A'(r_e)}} \right. \\
&\quad \left. + \frac{\sin \phi \sqrt{\frac{C(r_e)A'(r_e)}{A(r_e)C'(r_e) - C(r_e)A'(r_e)}}}{\sqrt{A(r_e)(\sin^2 \phi + B(r_e) \cos^2 \phi)}} \right) - 1, \quad (31)
\end{aligned}$$

where r_e is the orbital radius of the evolving massive particles, and the static observer is assumed to be located at infinity with the four velocity $U^\mu|_\text{d} = (1, 0, 0, 0)$.

Before proceeding, we should note that there exist three special azimuthal angles, i.e., $\phi = 0, \pm \frac{\pi}{2}$. Here $\phi = 0$ is assumed to be the opposite direction of the line of sight of the observer, and the observer is on the right-hand side of the black hole. Obviously, the impact parameter vanishes in this case and describes a photon emitted by an anticlockwise orbiting particle when moving at the location with the azimuthal angle $\phi = 0$. At this moment, the three velocity of the orbiting particle is perpendicular with respect to the line of sight of the distant observer, and the only contribution to the frequency shift of photons is the gravitational effect, which is defined by $z_{\text{tot}3} \equiv z_{\text{tot}}|_{\phi \rightarrow 0}$. Then, Eq. (25) shows that $\phi = \pm \frac{\pi}{2}$ corresponds to the minimum and maximum of the impact parameter, respectively. The minimal impact parameter describes the photon emitted by the anticlockwise orbiting particle when arriving at the location with the azimuthal angle $\phi = \frac{\pi}{2}$. At this moment, the initial three velocity of the photon is exactly opposite to the instantaneous orbital velocity of the particle. Thus, the redshift of the photon reaches the maximum defined by $z_{\text{tot}1} \equiv z_{\text{tot}}|_{\phi \rightarrow \pi/2}$. On the other hand, the maximal impact parameter describes the photon emitted by the evolving particle when reaching at the location with the azimuthal angle $\phi = -\frac{\pi}{2}$ and the initial three-velocity of the photon is the same as the instantaneous orbital velocity of the particle, which corresponds to the case of the maximal blueshift of the photon defined by $z_{\text{tot}2} \equiv z_{\text{tot}}|_{\phi \rightarrow -\pi/2}$.

Then, by defining the following variables,

$$R \equiv 1 + z_{\text{tot}1}, \quad (32a)$$

$$S \equiv 1 + z_{\text{tot}2}, \quad (32b)$$

$$T \equiv (1 + z_{\text{tot}3})^2, \quad (32c)$$

one can obtain two elegant closed formulas for the mass of the black hole and the quantum parameter in terms of these variables by inverting the relations (32) :

$$M = r_e \left(1 + \frac{\zeta}{T} - \frac{2\zeta}{RS} \right) \sqrt{\frac{3\zeta T}{15\zeta T - 4RS(2\zeta + T)}}, \quad (33)$$

$$A_\lambda = \frac{TR^2S^2(RS(2\zeta + T) - 3\zeta T)}{6\zeta(RS(\zeta + T) - 2\zeta T)^2}, \quad (34)$$

with $\zeta \equiv \frac{1+z_0}{1-z_0}$. These two formulas tell us that the mass of the black hole and the quantum parameter can be completely and independently given by few direct observables, i.e., the redshift $z_{\text{tot}1}$, blueshift $z_{\text{tot}2}$, and gravitational redshift $z_{\text{tot}3}$ of photons, as well as the orbital

radius r_e of the massive particle. It should be noted that the peculiar redshift z_0 is not a measurable quantity, but can be statistically estimated with the help of the direct observables and Eq. (31). Obviously, this general relativistic formalism described above can be used to predict the property of the compact object and probe the quantum effects precisely. To be specific, the compact object is a Schwarzschild black hole for $A_\lambda = 0$, a regular black hole for $0 < A_\lambda < \frac{1}{2}$, and a wormhole for $A_\lambda = \frac{1}{2}$. One can see Ref. [24] for more details.

In the following, we will give a brief analysis about the influences of the quantum effects and peculiar velocity on the frequency shifts of photons. Figure 1(a) shows that both of the redshift $z_{\text{tot}1}$ and the gravitational redshift $z_{\text{tot}3}$ decrease with A_λ . Besides, the blueshift also decreases with A_λ although the value of $z_{\text{tot}2}$ increases with it, since ω_d is in the denominator and the smaller ω_d means the larger $z_{\text{tot}2}$ but the smaller blueshift. In a word, the quantum effects reduce the frequency shifts of photons. The possible reason is that the quantum effects usually result in a weakening of the gravitational force [49]. What's more, Fig. 1(b) shows that the frequency shifts of the photons also decrease with the orbital radius r_e for fixed A_λ because the larger r_e is, the weaker the gravitational field becomes. Finally, Fig. 1(c) shows the frequency shifts versus the peculiar redshift or peculiar velocity. Obviously, the redshift $z_{\text{tot}1}$ and gravitational redshift $z_{\text{tot}3}$ increase with the radial receding peculiar velocity (corresponding to positive z_0) of the black hole with respect to the detector while the blueshift decreases with it although the value of $z_{\text{tot}2}$ increases. Besides, there exists a zero point for the blueshift since the kinematic effects is counteracted by the peculiar redshift at a particular receding velocity and similar zero point also respectively appears for the redshift and gravitational redshift at a particular approaching velocity (corresponding to negative z_0).

IV. THE PRESENCE OF PLASMA

In this section, we consider a more practical scenario, i.e., the black hole surrounded by a nonmagnetized, cold plasma, and investigate the effects of the plasma on the redshift/blueshift. The plasma is assumed as a static, inhomogeneous medium and the Hamiltonian for the photon in this plasma is given by [46, 47]

$$H = \frac{1}{2} [g^{\mu\nu} k_\mu k_\nu + \omega_p(r)^2], \quad (35)$$

where ω_p stands for the electron plasma frequency. By introducing the refractive index of the plasma medium

$$n^2 = 1 - \frac{\omega_p^2}{\omega^2}, \quad (36)$$

where ω stands for the frequency of photons measured by

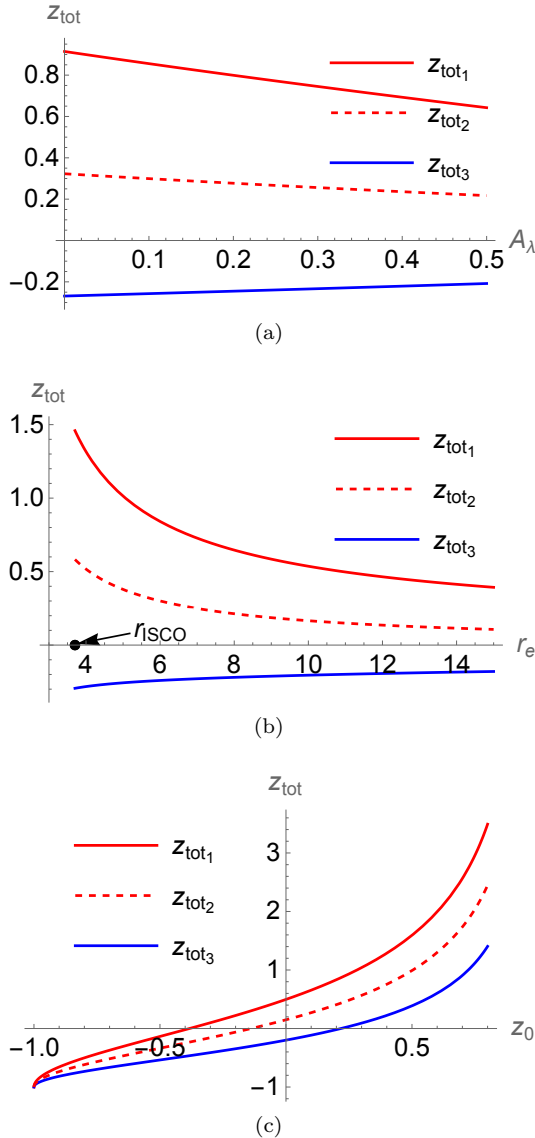


FIG. 1: The top panel plots the frequency shifts versus the quantum parameter A_λ with other parameters set to $M = 1$, $z_0 = 0$, and $r_e = 7$. The middle panel shows the frequency shifts versus the orbiting radius r_e with $M = 1$, $z_0 = 0$, and $A_\lambda = \frac{1}{3}$. The bottom panel shows the frequency shifts versus the peculiar redshift z_0 with $M = 1$, $r_e = 11$, and $A_\lambda = \frac{1}{3}$. Besides, all parameters are set to ensure $E^2 > 0$, $L^2 > 0$ and the stable condition (14) and r_e is larger than the radius of the innermost stable circular orbit (ISCO).

a static observer with respect to the plasma, the Hamiltonian can be rewritten as

$$\begin{aligned} H &= \frac{1}{2} [g^{\mu\nu} k_\mu k_\nu - (n^2 - 1)(k_\mu V^\mu)^2] \\ &= \frac{1}{2} g_{\text{eff}}^{\mu\nu} k_\mu k_\nu, \end{aligned} \quad (37)$$

where V^μ denotes the four velocity of the plasma, and $g_{\text{eff}}^{\mu\nu} \equiv g^{\mu\nu} - (n^2 - 1)V^\mu V^\nu$. Equation (37) shows that

photons travel along the geodesic in the effective metric $g_{\text{eff}}^{\mu\nu}$. Thus, for the case of a circular and equatorial orbiting massive particle, Eq. (26) can still be formally expressed as

$$1 + z = \frac{(E_\gamma U^t - L_\gamma U^\phi)|_e}{(E_\gamma U^t - L_\gamma U^\phi)|_d} = \frac{U_e^t - \hat{b}_e U_e^\phi}{U_d^t - \hat{b}_d U_d^\phi}, \quad (38)$$

with $\hat{b} \equiv \frac{L_\gamma}{E_\gamma}$. Although the definition is the same as the case of the absence of plasma, the impact parameter now incorporates the effects of plasma as explained in the following.

Considering the following plasma frequency with a radial power-law number density [46, 47]

$$\omega_p(r)^2 = \frac{4\pi e^2}{m} N(r), \quad N(r) = \frac{N_0}{r^h}, \quad (39)$$

where N_0 is a constant, and e and m respectively represent the electron charge and mass, the refractive index of the plasma medium can be expressed as

$$n^2 = 1 - A(r) \frac{k}{r^h}, \quad (40)$$

with $k \equiv \frac{4\pi e^2}{m\omega_0^2} N_0$ and ω_0 the frequency of the photon measured by a detector at infinity. For simplicity, we focus on the case of $h = 1$. Within this effective geometry, the energy and angular momentum for photons moving along the geodesics can be obtained as $E_\gamma = \frac{A}{n^2} k^t$ and $L_\gamma = C k^\phi$. Then, the equation of motion for photons at the equatorial plane can be given by

$$-\frac{n^2}{A} E_\gamma^2 + B(k^r)^2 + \frac{L_\gamma^2}{C} = 0. \quad (41)$$

Following the same procedure in the last section, the impact parameter can be calculated as

$$\hat{b} = -\frac{\sqrt{C} n \sin \phi}{\sqrt{A(\sin^2 \phi + B \cos^2 \phi)}}. \quad (42)$$

Obviously, the impact parameter incorporates the refractive index n of the plasma medium. Inserting the impact parameter into Eq. (38), the total frequency shift with the presence of plasma can be expressed as

$$\begin{aligned} \hat{z}_{\text{tot}} &= \sqrt{\frac{1+z_0}{1-z_0}} \left(\sqrt{\frac{C'(r_e)}{A(r_e)C'(r_e) - C(r_e)A'(r_e)}} \right. \\ &\quad \left. + \frac{n(r_e) \sin \phi \sqrt{\frac{C(r_e)A'(r_e)}{A(r_e)C'(r_e) - C(r_e)A'(r_e)}}}{\sqrt{A(r_e)(\sin^2 \phi + B(r_e) \cos^2 \phi)}} \right) - 1, \end{aligned} \quad (43)$$

where the static observer is also assumed to be located at infinity with the four-velocity $U^\mu|_d = (1, 0, 0, 0)$.

Similarly, one can also define three variables

$$\hat{R} \equiv 1 + \hat{z}_{\text{tot}1}, \quad (44a)$$

$$\hat{S} \equiv 1 + \hat{z}_{\text{tot}_2}, \quad (44\text{b})$$

$$\hat{T} \equiv (1 + \hat{z}_{\text{tot}_3})^2, \quad (44\text{c})$$

where $\hat{z}_{\text{tot}_1} \equiv \hat{z}_{\text{tot}}|_{\phi \rightarrow \pi/2}$, $\hat{z}_{\text{tot}_2} \equiv \hat{z}_{\text{tot}}|_{\phi \rightarrow -\pi/2}$, and

$\hat{z}_{\text{tot}_3} \equiv \hat{z}_{\text{tot}}|_{\phi \rightarrow 0}$. Then, two elegant closed formulas for the mass of the black hole and the quantum parameter can be derived from these variables by inverting the relations Eq. (44):

$$M = \frac{nr_e \left(\hat{T}n^2(\hat{T} - \zeta) + (\zeta + \hat{T})(\hat{R}\hat{S} - \hat{T}) \right)}{\hat{T} \left(\hat{R}\hat{S} - \hat{T}(1 - n^2) \right)} \sqrt{\frac{3\zeta\hat{T}}{\hat{T}n^2(7\zeta - 4\hat{T}) - 4(2\zeta + \hat{T})(\hat{R}\hat{S} - \hat{T})}}, \quad (45)$$

$$A_\lambda = \frac{\hat{T} \left(\hat{R}\hat{S} - \hat{T}(1 - n^2) \right)^2 \left(\hat{T}n^2(\hat{T} - \zeta) + (2\zeta + \hat{T})(\hat{R}\hat{S} - \hat{T}) \right)}{6\zeta \left(\hat{T}n^3(\hat{T} - \zeta) + n(\zeta + \hat{T})(\hat{R}\hat{S} - \hat{T}) \right)^2}. \quad (46)$$

In the following, we make a brief analysis about the effects of the plasma on the redshift/blueshift. To make the analysis clearly, we assume fixed ω_0 or ω_d , which is the natural frequency of the photon measured by a static observer located at infinity, and investigate the effects of the plasma on the frequency shifts through the emitting frequency ω_e . Figure 2 shows that both of the redshift and blueshift decrease with k , and there is a bound for the range of k since the photons cannot propagate in the region with $\omega_0 < \omega_p(r)\sqrt{A(r)}$. Besides, it should be noted that the plasma has no effects on \hat{z}_{tot_3} . The reason is that the impact parameter vanishes when the photon propagate radially along the line of sight of the observer, and Eq. (38) shows that the influence of the plasma vanishes when $\hat{b} \rightarrow 0$.

V. CONCLUSION

In this paper, we investigated the frequency shifts of photons emitted by massive particles revolving around a polymerized black hole, which is characterized by two parameters: the black hole mass M and the nonnegative parameter A_λ originated from quantum corrections. It is found that these two parameters can be completely and independently given by few direct astrophysical observables related to the frequency shifts of the photons. Then, we gave a brief analysis about the influences of the quantum effects on the frequency shifts. Besides, since plasma will change the behavior of the photon and most real black hole are surrounded by plasma, we studied the effects of the plasma on the frequency shifts of photons.

To be specific, for the case of a circular and equatorial orbiting massive particle, we computed the total frequency shift of the photons emitted by the massive particle. The total frequency shift z_{tot} includes three special cases, which respectively correspond to the max redshift z_{tot_1} for $\phi = \frac{\pi}{2}$, the max blueshift z_{tot_2} for $\phi = -\frac{\pi}{2}$, and the gravitational redshift z_{tot_3} for $\phi = 0$. By solving an

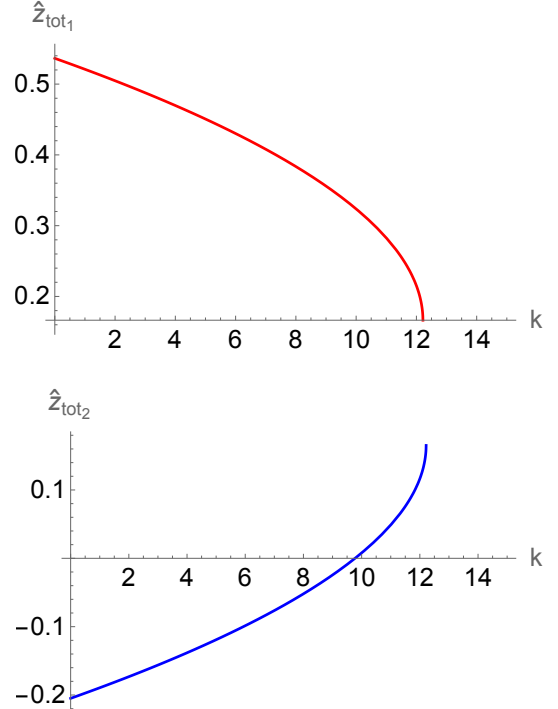


FIG. 2: The redshift (top panel) and blueshift (bottom panel) versus the parameter k with vanishing peculiar redshift $z_0 = 0$. The other parameters are set to $M = 1$, $r_e = 10$, and $A_\lambda = \frac{1}{3}$. All parameters satisfy $E^2 > 0$, $L^2 > 0$ and the stable condition (14).

inverse problem, we obtained two closed analytic expressions for the black hole mass and quantum parameter in terms of the redshift z_{tot_1} , blueshift z_{tot_2} and gravitational redshift z_{tot_3} , as well as the orbital radius r_e of the massive particle and the peculiar redshift z_0 which codifies the peculiar motion of the black hole. Namely, the mass of the black hole and the quantum parameter can be completely determined by few direct observables.

Besides, we found that all frequency shifts of photons decrease with the quantum parameter A_λ since the quantum effects weaken the strength of the gravitational field. The frequency shifts also decrease with r_e since the larger orbital radius means the weaker gravitational field. In addition, we investigated the frequency shifts versus the peculiar redshift and found that the redshift and gravitational redshift increase with the receding peculiar velocity of the black hole while the blueshift decreases with it. There exists a zero point for the blueshift where the kinematic effect is counteracted by the peculiar redshift at a particular receding velocity and similar zero point also respectively appears for the redshift and gravitational redshift at a particular approaching velocity.

Then, we investigated the refractive plasma effects on the frequency shifts of photons. After introducing an index of refraction of the plasma medium, the photons can still travel along the geodesic of an effective metric. Then, we calculated the frequency shifts of the photons following the same way as in the case of the absence of the plasma, and found that the black hole mass and quantum parameter also can be analytically solved in terms of the redshift \hat{z}_{tot_1} , blueshift \hat{z}_{tot_2} and gravitational redshift \hat{z}_{tot_3} . Besides, we analyzed the dispersion effects of the plasma and found that the frequency shifts always decrease with the plasma density.

Finally, we stress that this general relativistic formalism has been applied to a lot of Schwarzschild black holes

hosted at the core of different active galactic nucleuses, such as, NGC 4258 [50], TXS-2226-184 [51], J1346+5228 [52], and so on, where the authors estimate the mass-to-distance ratio of these black holes with a Bayesian fitting method by using the large data set of the frequency shifts of photons emitted by water masers orbiting them. In our forthcoming work, we will estimate the mass of the polymerized black hole hosted at different active galactic nucleuses and evaluate the quantum effects with the general relativistic formalism.

Acknowledgments

This work was supported by the National Natural Science Foundation of China (Grants Nos. 11975072, 11875102 and 11835009), the National Key R & D Program of China (Grants Nos. 2022SKA0110200 and 2022SKA0110203), the Liaoning Revitalization Talents Program (Grant No. XLYC1905011), the National Program for Support of Top-Notch Young Professionals (Grant No. W02070050), the science research grants from the China Manned Space Project (Grant No. CMS-CSST-2021-B01), the China Postdoctoral Science Foundation (Grant No. 2021M700729), and Shaanxi Provincial Education Department (Grant No. 21JK0556).

- [1] A. Ashtekar, T. Pawłowski, and P. Singh, *Phys. Rev. D* **74**, 084003 (2006).
- [2] A. Ashtekar and P. Singh, *Classical Quantum Gravity* **28**, 213001 (2011).
- [3] A. Corichi, T. Vukasinac, and J. A. Zapata, *Phys. Rev. D* **76**, 044016 (2007).
- [4] A. Ashtekar and M. Bojowald, *Classical Quantum Gravity* **23**, 391 (2006).
- [5] L. Modesto, *Classical Quantum Gravity* **23**, 5587 (2006).
- [6] M. Campiglia, R. Gambini, and J. Pullin, *Classical Quantum Gravity* **24**, 3649 (2007).
- [7] C. G. Boehmer and K. Vandersloot, *Phys. Rev. D* **76**, 104030 (2007).
- [8] D. W. Chiou, *Phys. Rev. D* **78**, 064040 (2008).
- [9] A. Corichi and P. Singh, *Classical Quantum Gravity* **33**, 055006 (2016).
- [10] J. Olmedo, S. Saini, and P. Singh, *Classical Quantum Gravity* **34**, 225011 (2017).
- [11] N. Bodendorfer, F. M. Mele, and J. Münch, *Classical Quantum Gravity* **36**, 187001 (2019).
- [12] N. Bodendorfer, F. M. Mele, and J. Münch, *Classical Quantum Gravity* **36**, 195015 (2019).
- [13] J. G. Kelly, R. Santacruz, and E. Wilson-Ewing, *Phys. Rev. D* **102**, 106024 (2020).
- [14] V. Faraoni and A. Giusti, *Symmetry* **12**, 1264 (2020).
- [15] W. C. Gan, N. O. Santos, F. W. Shu, and A. Wang, *Phys. Rev. D* **102**, 124030 (2020).
- [16] M. Bojowald, *Phys. Rev. D* **102**, 046006 (2020).
- [17] F. Sartini and M. Geiller, *Phys. Rev. D* **103**, 066014 (2021).
- [18] N. Bodendorfer, F. M. Mele, and J. Münch, *Phys. Lett. B* **819**, 136390 (2021).
- [19] N. Bodendorfer, F. M. Mele, and J. Münch, *Classical Quantum Gravity* **38**, 095002 (2021).
- [20] M. Bouhmadi-López, S. Brahma, C. Y. Chen, P. Chen, and D. Yeom, *J. Cosmol. Astropart. Phys.* **2007**, 066 (2020).
- [21] F. M. Mele, J. Münch, and S. Pateloudis, *J. Cosmol. Astropart. Phys.* **2202**, 011 (2022).
- [22] A. Arbey, J. Auffinger, M. Geiller, E. R. Livine, and F. Sartini, *Phys. Rev. D* **103**, 104010 (2021).
- [23] A. Arbey, J. Auffinger, M. Geiller, E. R. Livine, and F. Sartini, *Phys. Rev. D* **104**, 084016 (2021).
- [24] Q. M. Fu and X. Zhang, *Phys. Rev. D* **105**, 064020 (2022).
- [25] Y. L. Liu, Z. Q. Feng, and X. D. Zhang, *Phys. Rev. D* **105**, 084068 (2022).
- [26] S. Brahma, C. Chen, and D. Yeom, *Phys. Rev. Lett.* **126**, 181301 (2021).
- [27] J. B. Achour, S. Brahma, and J. Uzan, *J. Cosmol. Astropart. Phys.* **2003**, 041 (2020).
- [28] J. B. Achour and J. Uzan, *Phys. Rev. D* **102**, 124041 (2020).
- [29] J. B. Achour, S. Brahma, S. Mukohyama, and J. P. Uzan, *J. Cosmol. Astropart. Phys.* **2009**, 020 (2020).
- [30] K. Blanchette, S. Das, S. Hergott, and S. Rastgoo, *Phys. Rev. D* **103**, 084038 (2021).
- [31] J. Münch, *Phys. Rev. D* **104**, 046019 (2021).

- [32] Y. C. Liu, J. X. Feng, F. W. Shu, and A. Wang, Phys. Rev. D **104**, 106001 (2021).
- [33] A. Herrera-Aguilar and U. Nucamendi, Phys. Rev. D **92**, 045024 (2015).
- [34] M. Sharif and S. Iftikhar, Eur. Phys. J. C **76**, 404 (2016).
- [35] G. V. Kraniotis, Eur. Phys. J. C **81**, 147 (2021).
- [36] D. Ujjal, Chin. J. Phys. **70**, 213 (2021).
- [37] R. Becerril, S. Valdez-Alvarado, and U. Nucamendi, Phys. Rev. D **94**, 124024 (2016).
- [38] L. A. López and J. C. Olvera, Eur. Phys. J. Plus **136**, 64 (2021).
- [39] R. Becerril, S. Valdez-Alvarado, U. Nucamendi, P. Sheoran, and J. M. Dávila, Phys. Rev. D **103**, 084054 (2021).
- [40] U. Rashmi, N. Hemwati, and K. D. Purohit, Classical Quantum Gravity **35**, 025003 (2017).
- [41] P. Sheoran, A. Herrera-Aguilar, and U. Nucamendi, Phys. Rev. D **97**, 124049 (2018).
- [42] S. Komarov, A. Gorbatsievich, and A. Tarasenko, Gen. Relativ. Gravit. **50**, 132 (2018).
- [43] L. A. López and N. Bretón, Astrophys. Space Sci. **366**, 55 (2021).
- [44] A. Herrera-Aguilar, R. Lizardo-Castro, and U. Nucamendi, Astron. Nachr. **342**, 198 (2021).
- [45] P. Banerjee, A. Herrera-Aguilar, M. Momennia, and U. Nucamendi, Phys. Rev. D **105**, 124037 (2022).
- [46] A. Rogers, Mon. Not. Roy. Astron. Soc. **451**, 17 (2015).
- [47] V. Perlick, O. Yu. Tsupko, and G. S. Bisnovatyi-Kogan, Phys. Rev. D **92**, 104031 (2015).
- [48] F. Atamurotov and B. Ahmedov, Phys. Rev. D **92**, 084005 (2015).
- [49] R. R. Caldwell and D. Grin, Phys. Rev. Lett. **100**, 031301 (2008).
- [50] U. Nucamendi, A. Herrera-Aguilar, R. Lizardo-Castro, and O. L. Cruz, Astrophys. J. Lett. **917**, L14 (2021).
- [51] A. Villalobos-Ramírez, O. Gallardo-Rivera, A. Herrera-Aguilar, and U. Nucamendi, Astron. Astrophys. **662**, L9 (2022).
- [52] A. Villalobos-Ramírez, A. González-Juárez, M. Momennia, and A. Herrera-Aguilar, *A general relativistic mass-to-distance ratio for a set of megamaser AGN black holes II*, arXiv: 2211.06486.